SCEC 2007 Annual Report:
How does geometric complexity associated with the San Bernadino segment of the San Andreas influence slip distribution?

Michele Cooke and Laura Dair, University of Massachusetts

ABSTRACT

Numerical models simulate deformation of three alternative three-dimensional present-day configurations for the San Andreas Fault (SAF) through the San Gorgonio Pass. Models with north-dipping SAF better match uplift of the southern San Bernardino Mountains than a vertical SAF model. All models produce decreasing strike-slip rates southward along the San Bernardino strand of the SAF similar to geologic data. The models with north-dipping SAF better match the available strike-slip data. The north-dipping SAF model with continuous fault surfaces at depth has greater mechanical efficiency than the model with discontinuous echelon fault surfaces at depth. The complexity of the active fault geometry at the San Gorgonio Pass promotes the transfer of strike-slip from the San Andreas fault, to the nearby but not connected San Jacinto fault. We conclude that a north-dipping and continuous fault configuration is preferred for the San Andreas fault in the San Gorgonio Pass.

INTRODUCTION

In the San Gorgonio Pass (SGP) region, the right-lateral San Andreas fault (SAF) steps left in a contractional bend with complex, three-dimensional fault geometry (Fig.1; e.g. Matti et al. 1985). Although field investigations and seismicity reveal active north-dipping thrust fault surfaces through the SGP (e.g. Allen, 1957, Matti et al., 1992; Nicholson, 1996; Yule and Sieh, 2003; Carena et al., 2004), crustal deformation and earthquake rupture models simplify the SAF to be vertical through this region (e.g. Mead and Hager, 2005; Olsen et al, 2006; Smith and Sandwell, 2006). Within these simplified fault models, slip vectors are primarily strike-slip and the models neglect the reverse slip documented on the north-dipping San Gorgonio Thrust (Yule and Sieh, 2003). Without incorporating reverse slip, physical aspects of earthquake rupture dynamics and the regional seismic hazard may go uncharacterized. Consequently, models with geologically more realistic and complex geometry of the southern SAF may lead to more accurate assessment of earthquake hazards for southern California.

We use the Boundary Element Method (BEM) to numerically simulate crustal deformation of three different SAF configurations, through the San Gorgonio Pass. The BEM modeling technique uses a triangular mesh to accurately replicate three dimensionally irregular and complex fault surfaces. Using this mesh, we have developed the first dipping crustal deformation model of the southern SAF that incorporates geologically constrained and three-dimensionally irregular fault topology. Our study reveals the sensitivity of slip distribution and uplift pattern to SAF configuration. We compare the model results to geologic observations and offer a preferred fault configuration for the SAF through the SGP.

GEOLOGIC UPLIFT AND SLIP RATES

The SGP contains a complex network of strike-slip and thrust faults of which, only the incomplete surface traces are directly observable. Yule and Sieh (2003)

document a moderate north dip on the active San Gorgonio thrust (SGT). To the east, the SGT transitions into a more steeply north dipping strand of the SAF known as the Garnet Hill fault (Yule and Sieh, 2003). Furthermore, microseismicity in the region suggests that these faults maintain their north dip at depth (Carena, 2004). Both the observed and interpreted dip on these two faults refute the presence of a vertical through-going strand of the SAF within the SGP (Fig.1; Yule and Sieh, 2003; Carena, 2004).

Low-temperature thermochronometry at the Yucapia Ridge, located between the now inactive Mill Creek strand and the San Bernardino strand of the SAF, indicates ~3-6 km of uplift in the last 1.8 Ma (Spotila et al., 2001), giving a time averaged uplift rate of 1.6 – 3.3 mm/yr. Offset markers across the San Gorgonio thrust show 1 mm/yr relative uplift over the past 13 Ka (Yule and Sieh, 2003). Spatial variations in uplift rates are expected due to local fault geometry while temporal variations may reflect the complex evolution of the active strands of the SAF, such as proposed by Matti and Morton (1993).

Geolologic studies have revealed variable strike-slip rates along both the SAF and San Jacinto fault (SJF) within the SGP (Fig.1). Near the Cajon Pass, Weldon and Sieh (1985) found 24.5 ± 3.5 mm/yr strike-slip along the SAF (Fig.1 and 4). Southward, rates decrease along the San Bernardino strand to 11 – 16 mm/yr at Badger Canyon (McGill, 2007), to 3 – 17 mm/yr at Plunge Creek (McGill et al., 2006), and to 2.6 – 7.0 mm/yr at Burro Flats (Orozco, 2004). At Cabazon, where the San Bernardino strand intersects the SGT and Garnet Hill strand of the SAF the strike-slip rate decreases to 5.7 ± 0.8 mm/yr (Yule et al., 2001). At the Biskra Palms site, the Coachella segment of the SAF slips 9 – 15 mm/yr (Behr et al., 2007). Along the SJF, strike-slip rates vary from 13 – 18 mm/yr at site 7 (Fig.1; Kendrick, pers. comm.) to 7.2 -11.2 mm/yr at site 8 (Rockwell et al., 1990). In addition to strike-slip rates in the region, Yule and Sieh (2003) found a minimum of 2.5 mm/yr reverse-slip on the SGT.

SAF MODEL ALTERNATIVES

Three different fault geometries for the SGP were created based on the Southern California Earthquake Center Community Fault Model (CFM), a compilation of active faults in southern California (Plesch et al., 2007). The first end member model has a simplified, vertical fault geometry for the San Andreas and San Jacinto faults near the SGP. This model does not include the SGT but instead the San Bernardino strand transitions directly into the vertical Garnet Hill strand of the SAF (Fig.2 a). The second end member model follows the preferred configuration of the CFM (Plesch et al., 2007; Carena, 2004) and includes a discontinuous-at-depth SAF with moderately north-dipping Garnet Hill strand and SGT (Fig.2 b). The third intermediate model maintains the moderately dipping segments of the second end member but smoothly connects fault segments at depth (Fig.2 c). We describe these models as 1) a vertical SAF, 2) a north-dipping continuous SAF, and 3) a north-dipping discontinuous SAF model. In all models, the faults are freely-slipping and deformation is driven by 45 mm/yr of fault-parallel displacement at the edges of the model. The set-up of the models is further described in the supplement to this paper.

MODELED UPLIFT PATTERNS

The uplift maps reveal a significant difference between the vertical SAF model and the north-dipping SAF models (Fig. 4). The vertical configuration produces far less uplift than either of the north-dipping configurations. The north-dipping continuous model has the greatest uplift in the area of the San Bernardino Mountains (SBMs), with a maximum of 3 mm/yr relative to the surrounding region; however, the pattern and magnitude of uplift is difficult to distinguish from that of the north-dipping discontinuous model. These modeled uplift rates produced by the north-dipping fault models (~1-3 mm/yr) are comparable to geologic uplift rates for the southern SBMs (1.6-3.3 mm/yr; Spotila et al., 2001). In contrast, the vertical fault model produces only ~0.5-1 mm/yr of uplift relative to the surrounding area, and cannot account for the geologic uplift rates. In all models, subsidence > 1 mm/yr occurs within the San Bernardino Valley, which is consistent with depositional rates of 1-11 mm/yr in this valley (Carson et al., 1986).

SITE SPECIFIC GEOLOGIC SLIP RATES

We also compare the modeled slip rates at the Earth's surface with geologic rates obtained though specific paleoseismic and geomorphic studies (Fig. 4). The modeled strike-slip rates along the San Bernardino strand of the SAF decrease to the south and correlate well with geologic slip rates. However, the vertical SAF model overestimates right-lateral slip rates at several sites along the San Bernardino strand of the SAF (Fig.4). Again, the north-dipping fault configurations show a more favorable comparison to geologic observations than the vertical fault model. Additionally, the strike slip rates along the fault traces for the north dipping models are not significantly different from one another.

SLIP TRANSFER: SAF TO SJF

Right-lateral slip along the San Andreas fault is lowest for each model along the SGT/Garnet Hill strand, which is the area of greatest geometric complexity. This decrease in strike-slip rate along the SAF occurs at the same distance from the Cajon Pass as the greatest strike-slip rates along the San Jacinto fault (Fig.4). This suggests that, in the model, strike-slip is transferred from the SAF to the SJF even though the faults are not hard-linked. Within the models, the inefficiency of the constraining bend impedes strike-slip along the SAF and the SJF absorbs the excess strike-slip (Fig.4 and Table 1). Slip can transfer between two faults, with no physical structure connecting them, as the shear stresses are transmitted through the intervening material. When slip cannot be accommodated on a fault due to an inefficient geometry, some of that slip is taken up by other faults and the remainder becomes off fault deformation.

PREFERRED FAULT CONFIGURATION

While the vertical SAF model has greater mechanical efficiency than the models with north-dipping faults, the vertical SAF model fails to match the geologic uplift pattern, overestimates slip rates at several sites along the San Bernardino segment of the SAF, and neglects the geologic and seismic indications of active north-dipping faults in the SGP. Because both of the north-dipping fault models have similar uplift pattern and distribution of slip rates, our choice of fault configuration is based on the relative mechanical efficiency of the two models and our understanding of lower crustal

deformation. The north-dipping continuous model has greater mechanical efficiency than the discontinuous model. While the San Gorgonio fault is young and may be relatively inefficient, a discontinuous active fault geometry cannot be maintained within the lower crust. We expect that deformation deeper than ~10 km is continuous within geologic time scales and does not have patches of zero slip implied by discontinuous active fault surfaces. Of the three models, we favor the north-dipping, continuous fault geometry.

Our results suggest that models of crustal deformation in southern California that use only vertical faults will overestimate slip rates along the SAF in the SGP and underestimate off-fault deformation. These same models may also underestimate slip rates along the SJF, which accommodates some of the slip lost along the SAF through the SGP. The complexity of active faults through the SGP may influence earthquake rupture scenarios because regions of fault surface complexity may be regions where ruptures initiate, terminate, or jump to other faults (e.g. Harris et al., 1991; Wald and Heaton, 1994). Earthquake rupture along the southern San Andreas fault may produce significant ground shaking within the metropolitan Los Angeles region (Olsen et al, 2006). Consequently, the constraints on fault topology suggested here will help future rupture models of the southern San Andreas fault more accurately predict seismic hazards.

CONCLUSIONS

The San Andreas fault in the region of the San Gorgonio restraining bend is comprised of a complex network of dipping thrust and strike-slip faults. Incorporating geologic complexities, such as dipping fault surfaces into numerical fault models increases the match between modeled results and geologic observations. For example, the uplift of the San Bernardino Mountains is better matched by active north-dipping fault segments within the restraining bend than by a vertical San Andreas fault. Similarly, the north-dipping San Andreas fault models better match variable strike-slip rates at sites along the San Bernardino strand of the San Andreas fault. Although the north-dipping continuous San Andreas fault model and the north-dipping discontinuous San Andreas fault model produce similar results, the continuous model has greater mechanical efficiency and is preferred.

The San Andreas fault transfers strike-slip to the San Jacinto fault within the San Gorgonio Pass. The SJF picks up some of the strike slip that is lost to the San Andreas fault in an effort to by-pass the inefficient fault geometry within the San Gorgonio Knot. This transfer occurs between soft-linked faults that have no physical connection.

A paper on this work has been submitted to Geology and is currently under review. The paper is SCEC contribution number 1160.

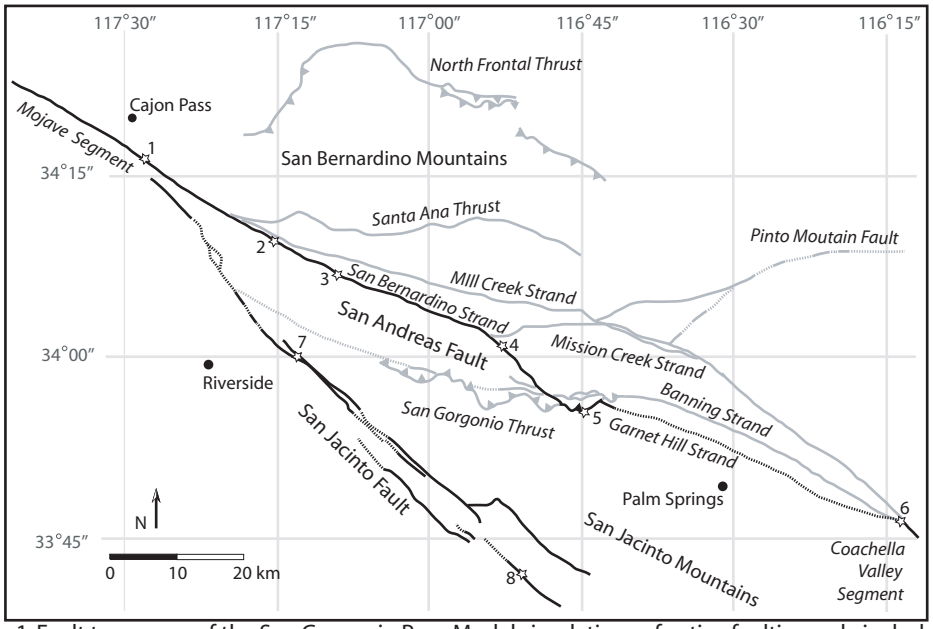

Fig.1. Fault trace map of the San Gorgonio Pass. Model simulations of active faulting only include the black faults. Stars indicate locations of geologic study sites that have yielded slip rates. The dashed lines indicate faults that have no surface trace. Site 1, Cajon Pass– Weldon and Sieh, 1985; site 2, Badger Canyon– McGill, 2007; site 3, Plunge Creek- McGill et al., 2006; site 4, Burro Flats – Orozco, 2004; site 5, Cabazon – Yule et al., 2001; site 6 - Behr et al., 2007; site 7 - Kendrick et al., 2002; site 8 - Rockwell et al., 1990 (modified from Matti and Morton, 1992).

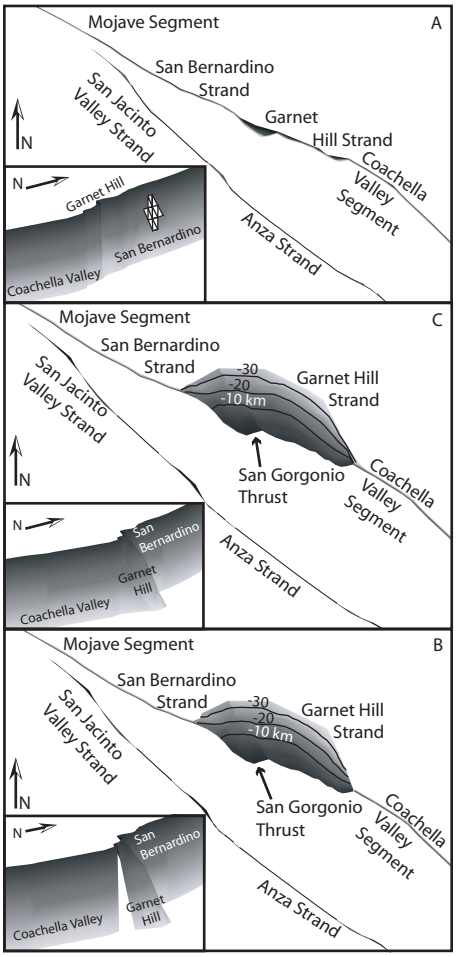

Fig.2. Map view of the A) vertical connected, B) dipping connected and C) dipping disconnected model fault geometries of active faulting through the San Gorgonio Pass. Darker shading indicates deeper depths to 35 km and structure contours are overlaid on dipping segments. The insert in each demonstrates the variations in connectedness at depth. The inset within A) also shows a section of the mesh used for all fault surfaces.

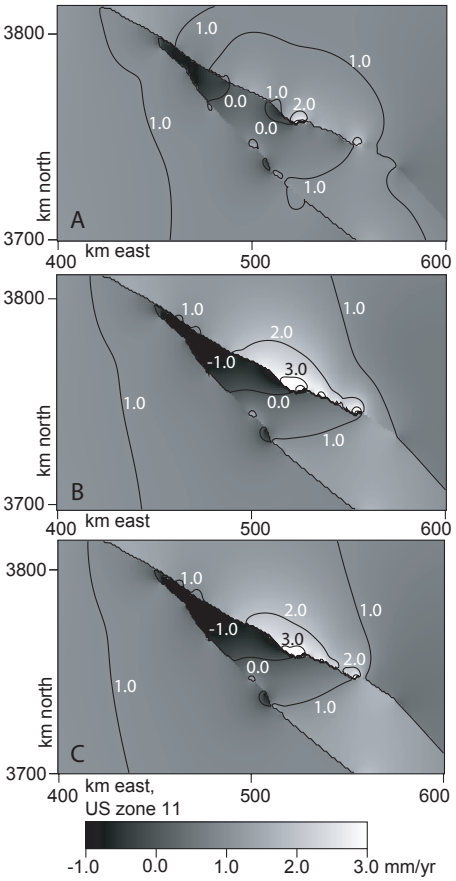

Fig.3. Uplift maps for each model. The vertical fault geometry does not show substantial localized uplift whereas the dipping models show uplift within the region of the southern San Bernardino Mountains. The dipping, continuous geometry shows the most uplift of the three models.

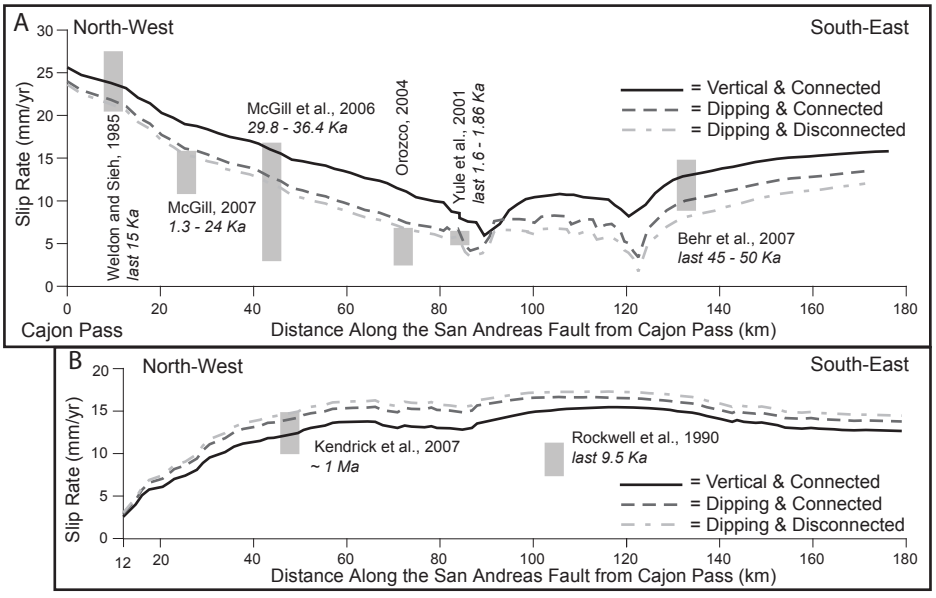

Fig.4. Strike-slip rates along the fault traces within the San Gorgonio Pass. The graphs have been arranged so that the scales are the same and positioned according to distance from Cajon Pass. The vertical, continuous model has the greatest right-lateral slip rate along the San Andreas fault but overestimates the geologic rates at three sites. This same model has the slowest strike-slip rates along the San Jacinto fault, indicating that more efficient configurations of the San Andreas fault have less slip partitioned to the San Jacinto fault.